

Spectral Edge Sensitivity in Neural Circuits of the Dorsal Cochlear Nucleus

Lina A. J. Reiss and Eric D. Young

Center for Hearing Sciences and Department of Biomedical Engineering, Johns Hopkins University School of Medicine, Baltimore, Maryland 21205

One possible function of the dorsal cochlear nucleus (DCN) is discrimination of head-related transfer functions (HRTFs), spectral cues used for vertical sound localization. Recent psychophysical and physiological studies suggest that steep, rising spectral edges may be the features used to identify HRTFs. Here we showed, using notch noise and noise band stimuli presented over a range of frequencies, that a subclass of DCN type IV neurons responded with a response peak when the rising spectral edge of a notch or band was aligned near best frequency (BF). This edge sensitivity was correlated with weak or inhibited responses to broadband noise and inhibition in receptive fields at frequencies below BF. Some aspects of the inhibition shaping the response peak, namely inhibition to rising edges below BF and to falling edges at BF, could be explained by the properties of type II interneurons with BFs below those of the type IV neurons. However, many type IV neurons also showed inhibitory responses with the rising spectral edge just above BF, and these responses could not be reproduced by current models of DCN circuitry. Therefore, a new component of the DCN circuit is needed to fully explain the responses to rising spectral edges. This shaping of edge sensitivity by inhibition to rising spectral edges both below and above BF suggests the specialization of DCN for spectral edge coding along the tonotopic gradient.

Key words: dorsal cochlear nucleus; spectral edges; spectral notches; sound localization; head-related transfer functions; DCN

Introduction

Spectral sound localization cues are created by the acoustic filtering properties of the outer ear; the frequency-specific changes in gain from the free field to a point near the eardrum are described by head-related transfer functions (HRTFs) (Blauert, 1969; Hebrank and Wright, 1974). In cats, HRTFs are characterized by a midfrequency notch, which shifts systematically in frequency with sound source azimuth and elevation (Musicant et al., 1990; Rice et al., 1992). This notch produces a sharp minimum in the sound spectrum at the eardrum, which is an important cue for vertical sound localization in cats (Huang and May, 1996; Tollin and Yin, 2003). Spectral notch processing has been associated with the dorsal cochlear nucleus (DCN) (Young and Davis, 2002; Oertel and Young, 2004) and interruption of the output axons of the DCN impairs the ability of behaving cats to orient to sound sources in the vertical plane (Sutherland et al., 1998; May, 2000).

Recent studies raise the question of whether it is the frequency of the notch itself or the frequency of the upper edge of the notch that is encoded. Psychophysical experiments in human observers show that steeply rising spectral edges can influence perceived

vertical location (Middlebrooks, 1992; Macpherson and Middlebrooks, 1999). Moreover, rising spectral edges are strongly encoded by type O neurons in the inferior colliculus (ICC) (Davis et al., 2003). Type O neurons receive a dominant excitatory input from type IV neurons in the DCN (Davis, 2001), and the edge sensitivity seen in the ICC could be derived from the DCN. Type IV neurons receive inhibitory inputs from type II interneurons with lower best frequencies (BFs) than the excitatory inputs to type IVs from the auditory nerve (AN) (Voigt and Young, 1990; Spirou and Young, 1991), an arrangement that could produce spectral edge sensitivity.

The goal of this study was to test whether DCN type IV neurons encode rising spectral edges and, if so, to determine whether the known circuitry of the DCN suffices to account for such encoding. Previous studies explored a different hypothesis, that spectral notches are encoded by inhibitory responses to the absence of energy in the notch, based on the finding that most type IV neurons are excited by broadband noise (BBN) but inhibited by notches centered on BF (Spirou and Young, 1991; Nelken and Young, 1994). These studies mainly examined the responses of DCN type IV neurons to notch noise with the notch centered on BF, which gives no information about encoding of notches with spectral edges at BF.

The data reported here show that the majority of DCN type IV neurons respond with a peak of discharge rate when a rising spectral edge is aligned near BF. This edge sensitivity is correlated with weak or inhibited responses to BBN and with inhibition in receptive fields at frequencies just below BF. Some aspects of the inhibition can be explained by the properties of known DCN inhibitory circuits; however, important aspects of the responses cannot be reproduced by the current model of the DCN (Han-

Received Dec. 6, 2004; revised Feb. 16, 2005; accepted Feb. 19, 2005.

This work was supported by National Institutes of Health Grants DC00115 and DC00441. Israel Nelken and Kevin Davis provided archival data, which was helpful for guiding the experimental protocol, as well as one onset-C unit shown in this paper. Ian Bruce provided the auditory nerve model used for dorsal cochlear nucleus simulations. We thank Sharba Bandyopadhyay, Steven Chase, Bradford May, and Israel Nelken for helpful comments on this manuscript.

Correspondence should be addressed to Eric D. Young, Department of Biomedical Engineering, Johns Hopkins University School of Medicine, 505 Traylor Building, 720 Rutland Avenue, Baltimore, MD 21205. E-mail: eyoung@bme.jhu.edu.

DOI:10.1523/JNEUROSCI.4963-04.2005

Copyright © 2005 Society for Neuroscience 0270-6474/05/253680-12\$15.00/0

cock and Voigt, 1999). Therefore, a new inhibitory component of the DCN circuit is needed to fully explain the responses to rising spectral edges.

Materials and Methods

Surgical procedures. Experiments were conducted on 22 adult cats (3–4 kg) with infection-free ears and clear tympanic membranes. Animal use protocols were approved by the Johns Hopkins Animal Care and Use Committee. A detailed description of the surgical procedures is provided by Nelken and Young (1994). Briefly, cats were tranquilized with xylazine (2 mg, i.m.) and anesthetized with ketamine (40 mg/kg, i.m.; supplemental dose, 15 mg/kg, i.m.). Atropine (0.1 mg, i.m.) was given to control mucous secretion. Cats were decerebrated by aspirating through the midbrain between the superior colliculus and thalamus, after which anesthesia was discontinued. Core body temperature was maintained at 38°C using a regulated heating blanket, and lactated Ringer's solution was given regularly to maintain fluid volume.

The DCN was exposed by drilling a small (~2 mm) hole through the bone ~3–5 mm lateral to the foramen magnum after removal of the occipital condyle (Young and Brownell, 1976). The DCN surface could be directly visualized after gentle parting of the choroid plexus, and no aspiration or retraction of neural tissue was needed for this approach. Recording electrodes were advanced into the DCN at an angle within 0–20° from the stereotaxic horizontal plane and ~10° azimuth, approximately perpendicular to its layers and at a slight angle to its isofrequency laminae. Single neurons were isolated and recorded extracellularly using platinum–iridium microelectrodes.

Acoustic stimuli and experimental protocol. Recordings were made in a sound-attenuating chamber. Acoustic stimuli were delivered to the ipsilateral ear via an electrostatic speaker coupled to a hollow ear bar. The speaker was calibrated *in situ* using a probe tube placed ~2 mm from the eardrum. The calibration was essentially flat, with fluctuations of <10 dB from 0.5–30 kHz.

Tones at the BF of the background activity or BBN were used to search for neurons along the track. Once a neuron was isolated, it was characterized using rate versus level functions for BF tones and BBN; stimuli were presented as 200 ms bursts once per second. Sound level was changed in 1 dB steps over an 80–100 dB range, and each level was presented once. Units were classified as type IV if they had moderate spontaneous rate and BF tone rate–level functions with excitation at low sound levels and inhibition (rate less than spontaneous rate) at high sound levels, as by Young (1984). Other units with moderate spontaneous rate and incomplete inhibition at high levels were classified as either type III or type IV-T, depending on whether the driven rate to BF tones at 35 dB relative to threshold was greater or less than half of the maximum driven rate, respectively (Shofner and Young, 1985). Units were classified as type II neurons if they had no spontaneous rate and strongly excitatory but nonmonotonic responses to BF tones, but little response to BBN (<30% of maximum BF tone rate). Only neurons located along the electrode track before a change in the direction of the BF gradient, which indicates a transition from DCN to ventral cochlear nucleus (VCN), were classified as DCN neurons. In VCN, at depths after a BF gradient shift,

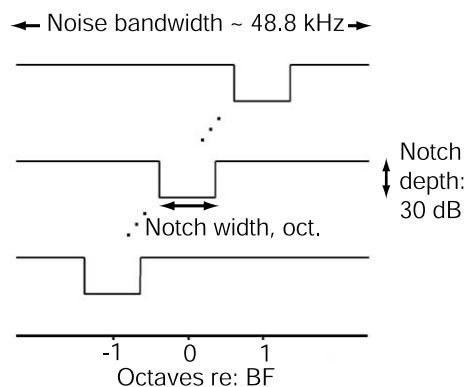


Figure 1. Notch noise center frequency sweep set. Stimuli were symmetric and had constant notch width in logarithmic frequency space, as shown. Across sets, notch widths were varied as $1/32$, $1/16$, $1/8$, $1/4$, $1/2$, 1, or 2 octaves (oct.). One hundred stimuli were presented with center frequencies from –1 to 1 octaves relative to (re): BF. Noise band center frequency sweep sets were similar, with bandwidths and sound levels varied.

units were classified as onset-C neurons if they had onset responses to tones, no spontaneous rate, and strong BBN responses.

Response maps were collected for many neurons. They were constructed by recording responses to 200 ms tone bursts presented once per second over a range of frequencies (usually 100 tones spaced over 2 octaves centered on BF) and sound levels (40–80 dB range in 10 dB steps). Each frequency–sound level combination was presented once, starting from BF and progressing to alternately lower and higher frequencies at each sound level. In the absence of spontaneous activity, response maps were collected in the presence of a second tone fixed at BF 3–8 dB above threshold to produce background activity and reveal inhibitory effects.

Once a neuron was characterized, notch noise and noise band sweep sets were presented. Notch noise stimulus spectra were defined in the frequency domain, each with 48.8 kHz bandwidth, infinite edge slopes, and notch depths of 30 dB, shown in Figure 1. Each notch sweep set consisted of 100 notch noise stimuli with logarithmically constant notch widths and notch center frequencies ranging from 1 octave below to 1 octave above BF in $\sim 1/50$ octave steps. For BFs >24.4 kHz, the highest notch frequencies presented were <1 octave above BF because of sampling rate limitations. Noise band sweeps were similar, except that the center frequency of the band was varied in place of the notch. Across sets, notch (band) width was varied as $1/32$, $1/16$, $1/8$, $1/4$, $1/2$, 1, and 2 octaves.

These stimulus spectra were corrected for irregularities in the sound-system transfer function using the inverse of the speaker calibration. The frequency spectrum of each stimulus was sampled with 32,768 points and inverse Fourier transformed with random phase to create ~335.5 ms stimulus bursts in the time domain (sampling rate of 97,656.25 Hz). The same set of random phases was used for all sweep stimuli. Linear 10 ms ramps were added to the onset and offset of the stimuli. All stimuli at a

Table 1. Changes in DCN circuit connectivity parameters from the model of Hancock and Voigt (1999)

Input population → target	Frequency offset C_{AB} (octave)	Integration bandwidth BW_{AB} (octave)	Number of inputs × synaptic weight $N_{AB} \times g_{AB}$
AN → T2	0.0	0.2	23.1 (26.1)
AN → WBI	0.0	2.0 ^{a,b} (3.0)	10.8 (8.4)
AN → T4	0.0	0.24	2.75 (4.8)
WBI → T2	0.3 ^a (0.0)	0.05	7 (21)
WBI → T4	0.05	0.1	0–19.8 ^a (9)
T2 → T4	–0.1 ^a (0.0)	0.2	47.25
NSA → T4	N/A	N/A	0.7

Original values are shown in parentheses when they have been changed. Input population parameters: C_{AB} is the frequency offset of the input population from the target cell; BW_{AB} is the integration bandwidth of the input population; N_{AB} is the number of cells in the input population bandwidth [unlike by Hancock and Voigt (1999), N_{AB} is determined by the bandwidth as one input unit per 1/100 octave]; g_{AB} is the synaptic strength of the input population relative to the resting conductance of the cell. Because the product $N_{AB} \times g_{AB}$, and not g_{AB} alone, determines the net effect of each input population, only $N_{AB} \times g_{AB}$ is shown for comparison with original values. N/A, Not applicable; T2, type II; T4, type IV; NSA, nonspecific afferent.

^aThese changes had the largest effect on model behavior.

^bBandwidth is effectively 2.0 because of Gaussian-distributed weighting of inputs >3.0 octaves, with the largest weights concentrated over a 2.0 octave bandwidth.

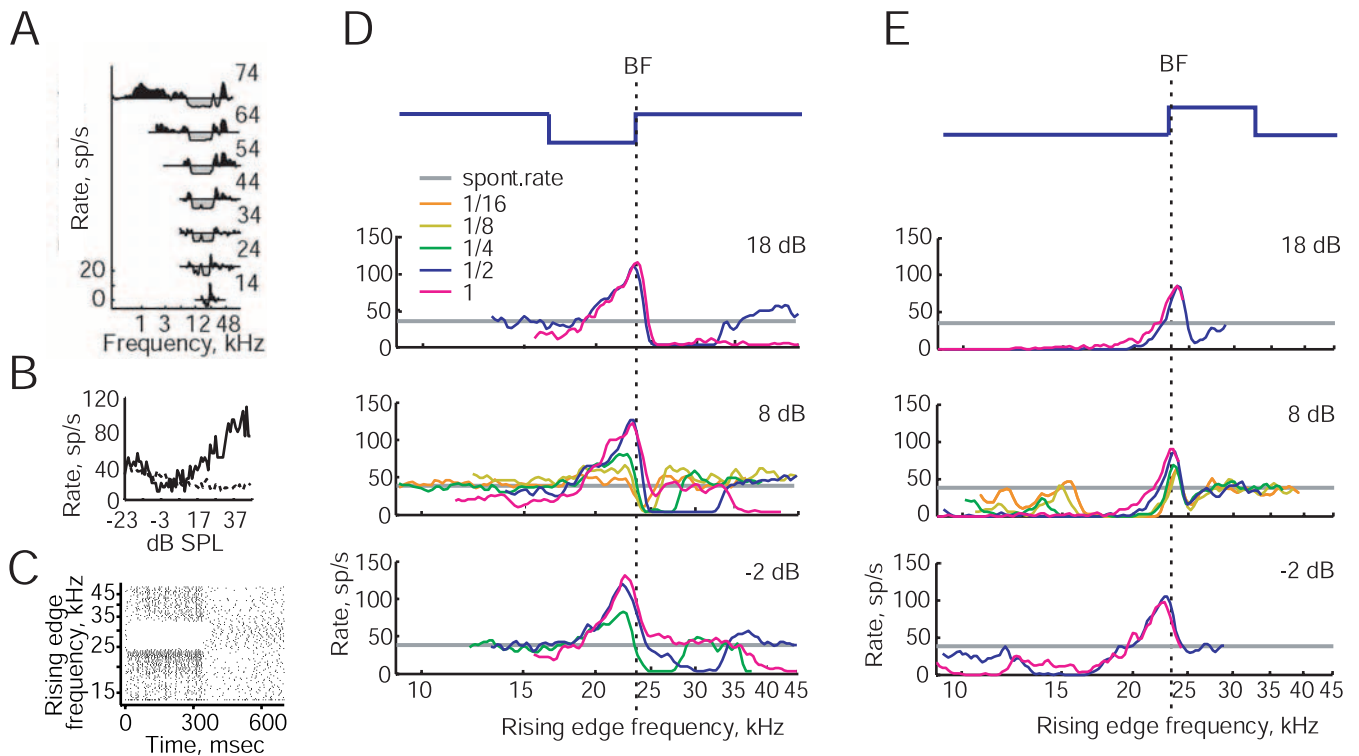


Figure 2. Unit with a large peak of discharge rate when the rising edge of the notch noise or noise band was near BF (BF of 23.3 kHz). **A**, Tone response map. Sound levels are labeled in decibels of sound pressure level (dB SPL) at the BF; actual levels vary with the calibration. Rates are plotted as rate relative to spontaneous. sp/s, Spikes per second. **B**, Rate versus level function for BBN. Levels are the spectrum level in decibels relative to $20 \times 10^{-6} \text{ Pa}/(\text{Hz})^{1/2}$ at BF. The BBN was not compensated for the acoustic calibration. The dotted line is the rate during the interstimulus interval after the stimulus. **C**, Example dot raster plot for notch noise with a notch width of $1/2$ octave presented at a spectrum level of 8 dB. Rate responses to notch noise sweep sets (**D**) and noise band sweeps (**E**) are shown for different notch widths or bandwidths (colors) and sound levels (rows). Levels are spectrum level in the pass band in decibels relative to $20 \times 10^{-6} \text{ Pa}/(\text{Hz})^{1/2}$. The horizontal gray line is spontaneous rate (spont. rate) measured from rate–level functions at subthreshold levels. Rates were smoothed by convolution with a three-point triangular window. The top plot shows the stimulus spectrum at the peak discharge rate for the $1/2$ octave notch or band.

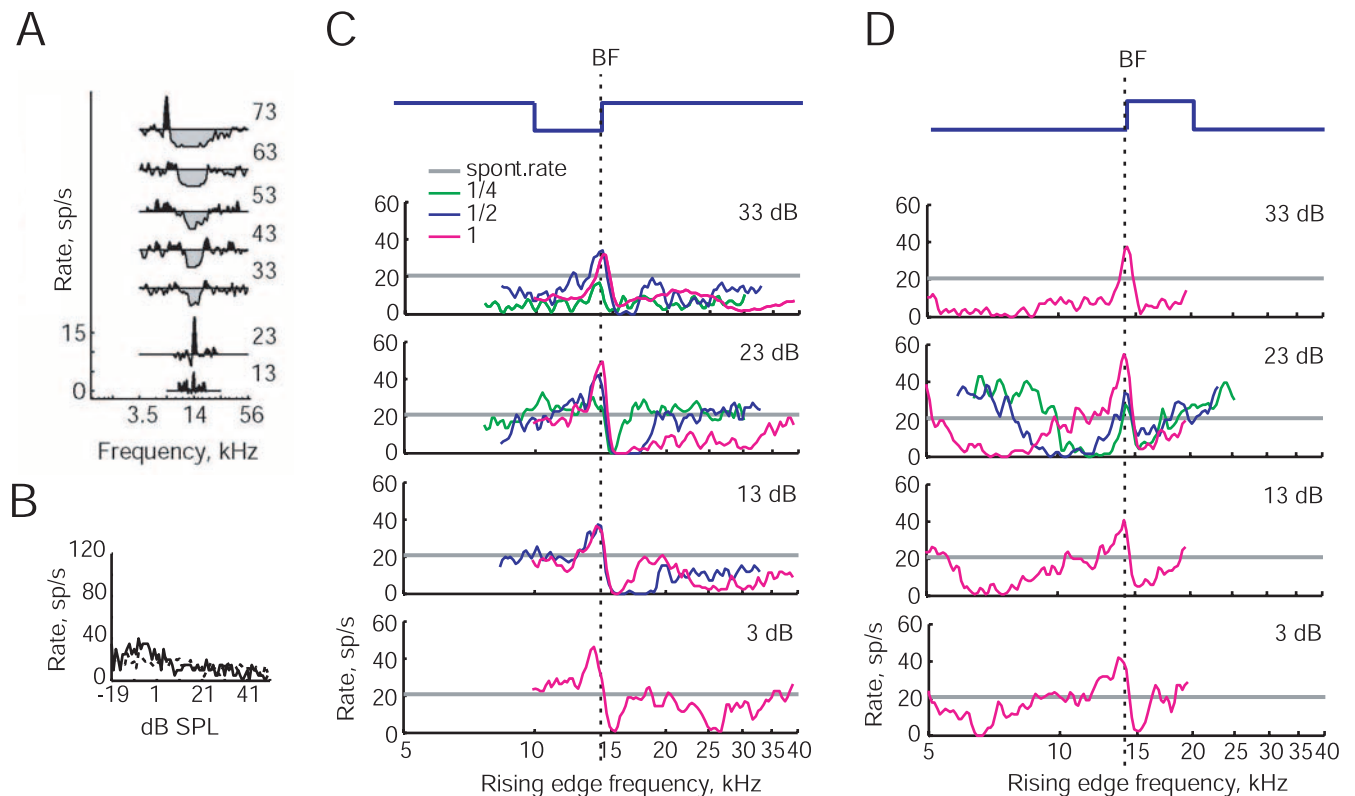


Figure 3. Unit with a smaller peak and lower background rate than Figure 2 (BF of 14.0 kHz). Organized as in Figure 2, except that no dot raster is shown. dB SPL, Decibels of sound pressure level; sp/s, spikes per second; spont. rate, spontaneous rate.

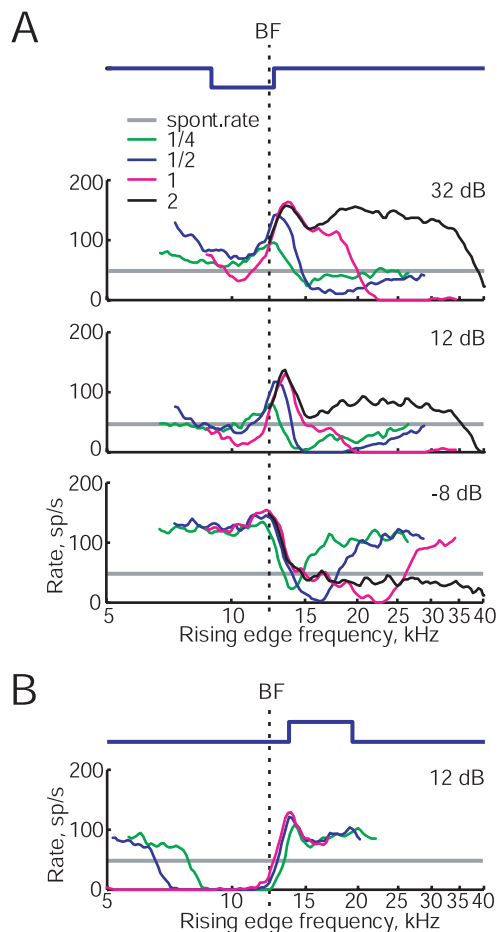


Figure 4. Unit with a peak that broadened and shifted with sound level and notch width (BF of 12.3 kHz). **A** and **B** are organized as in Figure 3, *C* and *D*. *sp/s*, Spikes per second; *spont. rate*, spontaneous rate.

given sound level were presented with the same pass-band spectrum level; hereafter, for notch noise or noise band stimuli, the notation “dB” in the text will represent the spectrum level of the pass band in decibels relative to $20 \text{ Pa}/(\text{Hz})^{1/2}$.

The stimuli were presented once per second, sequentially from the lowest notch (band) center frequency to the highest center frequency. The first stimulus was presented an additional 10 times to preadapt the neuron. The stimuli were presented over a range of sound levels, spaced at 10 dB, from just above BBN threshold to the maximum speaker output level. Rate responses were averaged over the stimulus duration.

Simulations using the DCN model. Responses of onset-C, type II, and type IV neurons were simulated in Matlab (MathWorks, Natick, MA) with a model based on the one developed by Hancock and Voigt (1999). The model circuit was the standard DCN model proposed by Young and colleagues, shown in Figure 12*D* (Young and Davis, 2002); the wide-band inhibitor (WBI) in the circuit was assumed to be the onset-C cell of the VCN (Nelken and Young, 1994; Winter and Palmer, 1995). Similar intrinsic and connection parameters were used as by Hancock and Voigt (1999), except for the following changes: b_k , a parameter governing the effect of the variable potassium conductance, was set to 10 instead of 2 for the type IV and WBI cells and 9 instead of 1.75 for the type II cells; the BFs of certain input populations were offset to lower or higher frequencies relative to the BFs of their target cells, as described in Results; and finally, a Gaussian instead of flat distribution of synaptic weights was used for each population of connections. The Gaussian distribution was shaped to have an SD equal to half of the original bandwidth of Hancock and Voigt (1999) for each population, except for the AN inputs to the WBI, in which a relatively smaller SD equal to one-third of the original integra-

tion bandwidth was used. Changes to the connectivity parameters are described fully in Table 1 and discussed further in Results.

AN inputs to the model were simulated with a model developed by Bruce et al. (2003) for complex, broadband sounds and based on the previous model of Zhang et al. (2001). Because the Bruce model is only valid for high spontaneous rate fibers, simulations were restricted to low sound levels in the middle of the dynamic range of these fibers for broadband stimuli, at approximate pass-band levels of 0 dB. This was necessary because both real (Hellstrom, 1998) and simulated high spontaneous rate fibers start to saturate for notch noise at pass-band levels of 10 dB and higher, eliminating the ability to code spectral features, in contrast to the obvious coding of spectral features by real DCN neurons at high levels. In reality, DCN neurons most likely compensate for saturation by integrating high and low spontaneous rate AN fiber inputs, which cannot be done with the current model.

AN responses to tones, BBN, and notch noise were simulated for AN BFs spaced at $1/100$ octave over a range of 4 octaves centered on 2.5 kHz (i.e., frequencies within the validated range for the model). This wide BF range was required for integration over at least 3 octaves by onset-C neurons. To reduce the scatter in responses to notch noise and noise bands, AN responses at each BF were simulated 10 times and saved, and the input to the model was taken as the average of 10 repetitions randomly selected from this set, with replacement. All other inputs (type II and onset-C) and stimuli (tones, BBN, and HRTFs) were simulated just once at each BF.

Results

Type IV units with peak responses to rising spectral edges

We found that 24 of 37 (65%) type IV neurons were selective for rising spectral edges (i.e., they exhibited a single excitatory peak response) in notch noise and noise band sweeps, for stimuli with the rising spectral edge aligned near BF. The remaining 13 of 37 (35%) type IV neurons lacked this peak to the rising edge, although they may have had a small peak to the falling edge or when the notch noise was centered on BF. Figures 2–4 show the rate responses of three type IV neurons that illustrate the range of responses in edge-sensitive units. In each figure, different colors represent different notch or bandwidths, and sound levels increase from the bottom to top rows.

The two examples in Figures 2 and 3 illustrate the edge sensitivity seen in the majority of type IV neurons. For the notch noise sweeps shown in Figures 2*D* and 3*C*, these neurons showed a peak response with the rising spectral edge aligned near BF; the stimulus eliciting the peak response is shown at the top. The example in Figure 2 had a large peak rate of >100 spikes per second, and the example in Figure 3 had a smaller peak rate just above spontaneous rate (gray line) with a larger contribution of inhibition in the shaping of the peak, especially at high sound levels. In units like these examples, there was a strong inhibition of response for the notch edge frequencies above BF (i.e., for the BF within the notch). The range of notch frequencies over which the inhibition was seen broadened with increasing notch width, although the inhibition was usually strongest for rising edge frequencies just above BF (Fig. 3*C*). The overall background rate also often decreased with notch width; this was particularly apparent at frequencies below the peak rising edge frequency (Fig. 2*D*).

The example in Figure 4 shows a second kind of notch response that was observed in some edge-sensitive neurons. These neurons showed a large peak response to notch noise with the rising edge at or slightly above BF (Fig. 4*A*) but lacked the inhibitory response for rising edge frequencies just above BF, as in Figures 2 and 3. This unit showed inhibitory responses to rising edge frequencies farther above BF for narrow notch widths and low sound levels, but these responses became excitatory as notch width broadened or sound levels increased.

Several qualitative features were similar across edge-sensitive neurons. These examples show that changes in sound level had little effect on the peak height, although the peak location shifted slightly upward in frequency with increasing sound level, especially for units like the one in Figure 4. Conversely, notch width had a large effect on the peak height, because the peak was diminished at notch widths of $\frac{1}{4}$ octaves or smaller, best seen in Figures 2*D* and 4*A*.

For noise band sweeps (Figs. 2*E*, 3*D*, 4*B*), most (16 of 18 units with noise band data, 89%) notch-edge-sensitive neurons also responded maximally to noise bands with the rising spectral edge aligned near BF; again, the stimulus eliciting the maximum rate is shown at the top of the figure. Like the peak seen in notch noise sweeps, the peak rate for noise band sweeps was invariant with sound level, although the peak location shifted upward slightly with increasing sound level. The bandwidth had little or no effect on peak size. The common feature between the optimal notch and band stimuli is the steep rising spectral edge near BF, which implies that the spectral edge is the feature that is encoded by these neurons.

The population of edge-sensitive units could be divided into two groups by the presence or absence of inhibition with the rising edge above BF (criterion: the rate is below or above spontaneous rate for rising edge frequencies within 0.2 octaves above BF for the $\frac{1}{2}$ octave notch width sweeps). These are called low-rate (units like those in Figs. 2, 3) and high-rate (Fig. 4) below. Population data for the two groups are shown in Figure 5. The group with inhibition for the rising edge above BF, the low-rate group (16 of 24, 67%) (Fig. 5*A*, brown), showed sharp peaks of response to rising spectral edges; the peaks were similar at different notch widths and sound levels. The group without inhibition, the high-rate group (8 of 24, 33%) (Fig. 5*A*, green), showed more variability in response as the stimulus changed. The stability in low-rate units is apparently attributable to the strong inhibition to rising spectral edges just above BF. This additional inhibition may also be responsible for the lower overall rate response.

Other differences between these two subgroups became apparent when notch width or sound level was varied. The peak location varied more as notch width changed for the high-rate group, as shown for mean population responses in Figure 5*B*. A similar effect was observed for noise band sweeps, in which the peak shifted to higher frequencies with decreasing bandwidth (data not shown). This peak shift across notch widths was more apparent at intermediate to high sound levels (Fig. 5*C*, thick green lines) than at low sound levels (Fig. 5*C*, thin green lines).

When sound level was varied, both low-rate and high-rate units showed shifts in peak location to higher frequencies with increasing sound level, as shown in Figure 5*C* for two notch widths. The shift was especially apparent between very low and

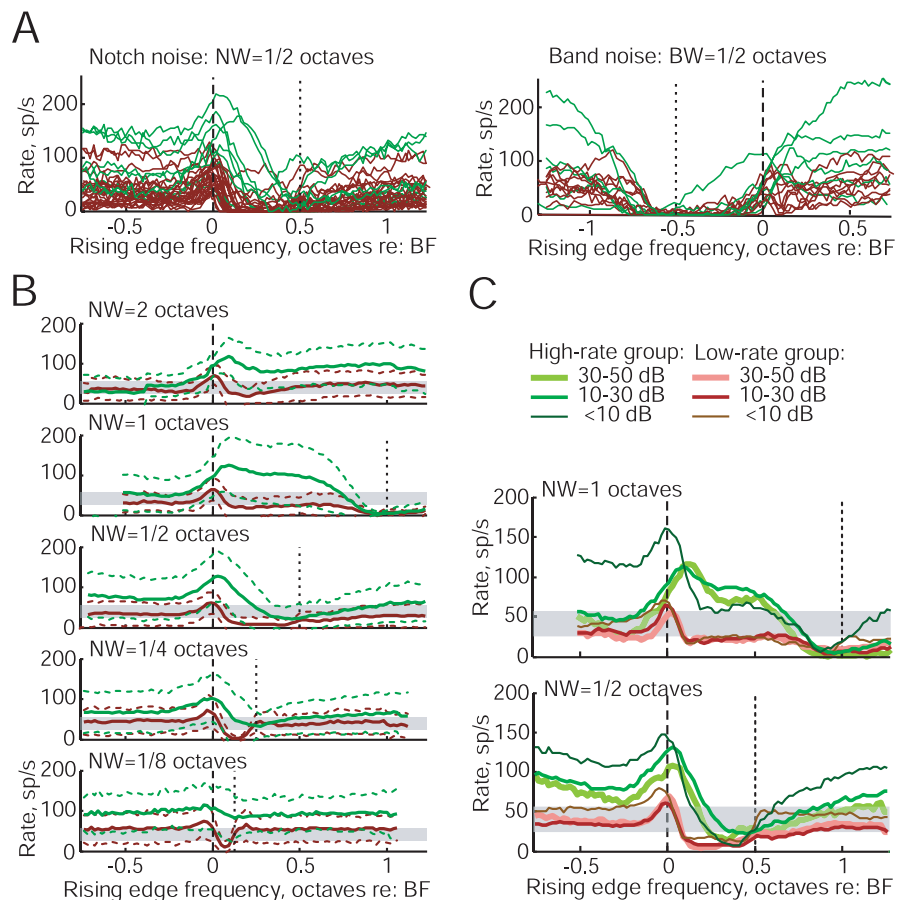


Figure 5. Superimposed and average population responses of edge-sensitive type IV units to notch and band noise sweeps presented at pass-band levels of 10–30 dB. All responses are superimposed and averaged with the *x*-axis normalized to octaves relative to BF. **A**, Superimposed notch noise sweep responses (left) and band noise sweep responses (right) show two subgroups of edge-sensitive units: a low-rate group (brown) and a high-rate group (green). The groups are defined based on notch responses only. **B**, Mean responses to notch noise at various notch widths show peaks that shift to higher edge frequencies with increasing notch width, notably for the high-rate group. Dashed lines indicate 1 SD above and below the mean. The area shaded light gray indicates the range of spontaneous rates (within ± 1 SD of the mean). **C**, Mean responses to notch noise at various sound levels show peaks that shift to higher frequencies with increases in sound level, again more so for the high-rate group. NW, Notch width; BW, bandwidth; sp/s, spikes per second; re., relative to.

intermediate sound levels. However, the high-rate group had larger shifts than the low-rate group, especially evident for notch widths of 1 octave.

Units without spectral edge sensitivity

The remaining type IV neurons, which lacked the peak to the rising edge, could be divided into three groups; the majority (8 of 13) showed no excitatory peak at all; 1 of 13 responded to falling edges; and 4 of 13 were excited instead of inhibited by notches centered on BF.

The neurons of the first group, like the edge-sensitive neurons, were inhibited by notch noise centered on BF (Fig. 6*C*); we call these notch-inhibited units. As for edge-sensitive units, the width of inhibition broadened for wider notch widths. Unlike edge-sensitive neurons, the background rate remained substantially above spontaneous rate and was not affected by notch width. These neurons were excited by noise bands centered at BF, and the width of excitation broadened for wide bandwidths (Fig. 6*D*). Some neurons in this group were inhibited by noise bands centered at BF for narrow, but not wide, bandwidths. This dichotomy corresponds to a transition from inhibition for narrow-

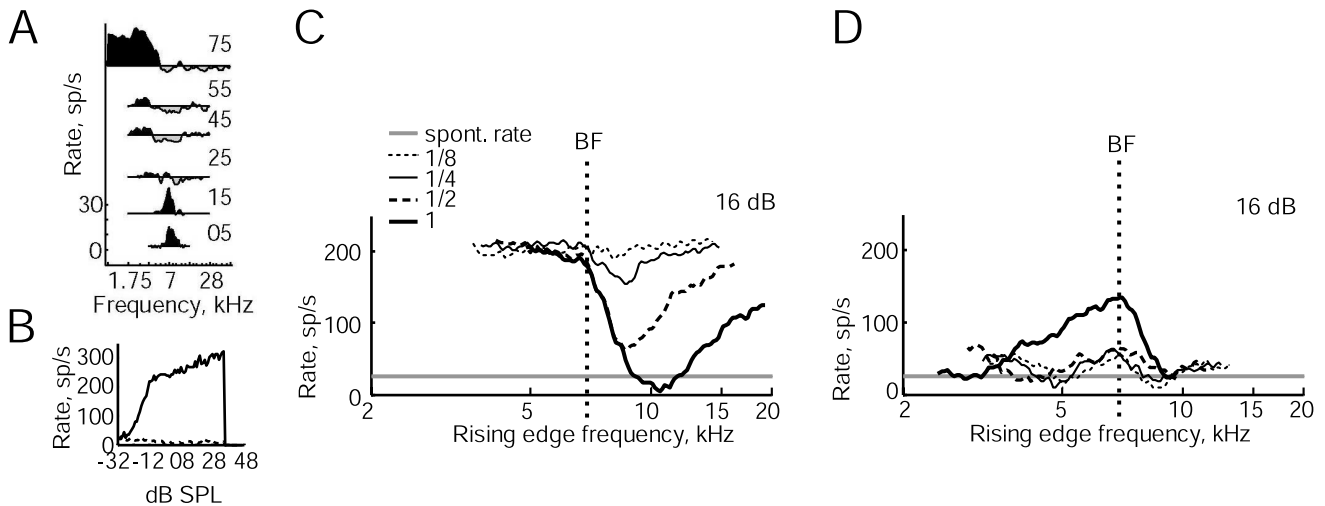


Figure 6. Non-edge-sensitive unit of the notch-inhibited type (BF of 6.9 kHz). Organized as in Figure 3. dB SPL, Decibels of sound pressure level; sp/s, spikes per second; spont. rate, spontaneous rate.

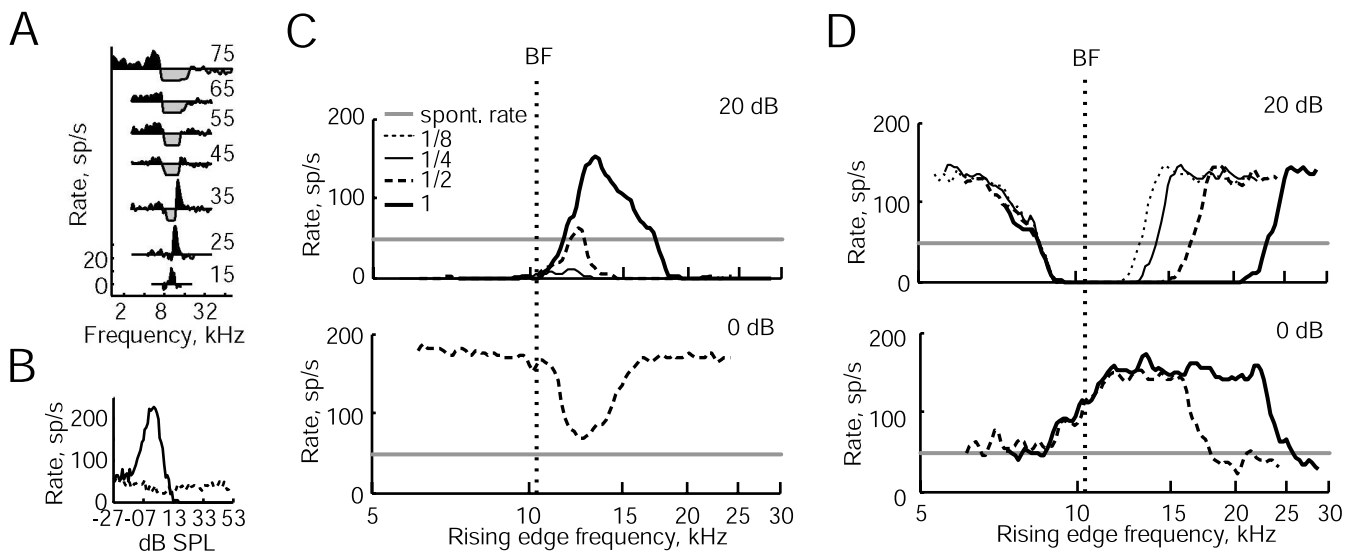


Figure 7. Non-edge-sensitive unit of the notch-excited type; the unit was excited by notches at BF at pass-band spectrum levels of 20 dB or greater (BF of 10.3 kHz). Organized as in Figure 3. dB SPL, Decibels of sound pressure level; sp/s, spikes per second; spont. rate, spontaneous rate.

band stimuli to excitation for broadband stimuli (Nelken and Young, 1994). The transition bandwidth varied from unit to unit, and sometimes responses were excitatory to the smallest bandwidth tested as in the example shown.

Figure 7C shows an example from the four units that were excited by notches at or just below BF; we call these notch-excited units. Two units were recorded at low sound levels below spectrum levels of 20 dB, and these units behaved like the notch-inhibited group in that they were inhibited by notches centered on BF. At higher sound levels, four of four units were excited instead of inhibited by notches centered on BF, and the excitatory response broadened with notch width. The maximum rate also increased with increasing notch width. The responses with the notch away from BF were either completely inhibited (two of four units) (Fig. 7C) or weakly influenced (two of four units) (data not shown).

Figure 7D shows a similar trend for noise band sweeps. At low sound levels, units were excited by noise bands centered on BF. At high sound levels, responses were inhibited by noise bands centered at or just below BF and strongly excited elsewhere. This

excitation to noise bands centered far away from BF does not necessarily mean that there are excitatory inputs far away from BF but is more likely attributable to the strongly non-monotonic BBN rate–level function and represents a response to the energy in the stop band of the noise, which is 30 dB down from the pass band. For the example in Figure 7, a noise band with a pass-band level of 20 dB will have a stop-band level of -10 dB; a noise band centered on BF will be inhibitory because the neuron is inhibited by BBN at 20 dB (Fig. 7B). However, when the noise band is far from BF, the neuron will be excited by the stop-band at BF because the neuron is excited by BBN at -10 dB. The same argument applies for notch noise centered on BF.

Type III and type IV-T units were also recorded in the DCN and were generally found to be non-edge sensitive, responding like the notch-inhibited type IV unit in Figure 6. Of the type III units, three of four were notch inhibited, and one of four had a small peak to falling spectral edges. Of the type IV-T units, three of five were notch inhibited, one of five had a small peak to rising spectral edges, and one of five had a small peak to falling spectral edges.

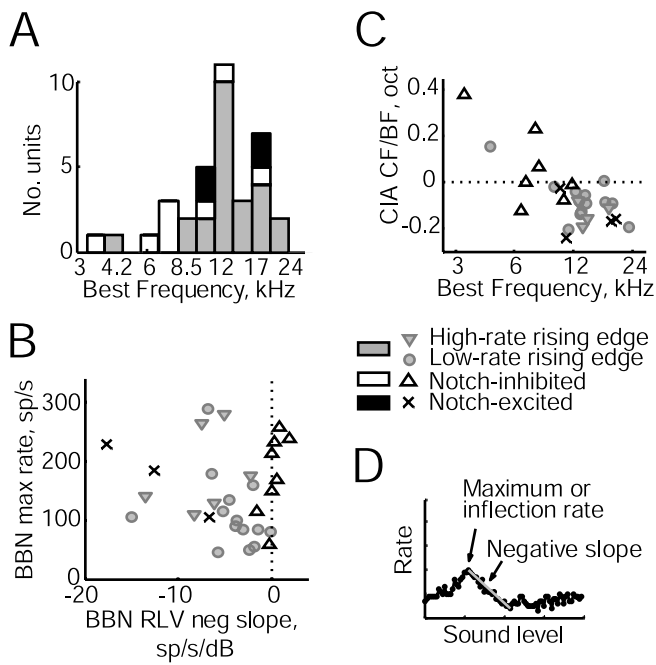


Figure 8. Tone and noise response properties for edge-sensitive versus nonsensitive units. **A**, BF distributions. **B**, Rate at the inflection or maximum point of BBN rate functions plotted versus the slope of the same functions, measured as in the plot in **D**. Four edge-sensitive units and one notch-excited unit with negative slopes that changed over time were excluded. **C**, Frequency offsets between the inferred CIA CF and the excitatory BF. Units without sufficient sampling of tone levels were excluded because CIA CF could not be adequately estimated. **D**, Broadband noise rate versus sound level function, illustrating the inflection or maximum rate and the negative slope, measured as indicated by the arrows. oct, Octave; neg, negative; sp/s, spikes per second; RLV, rate–level function.

What other properties distinguish edge-sensitive and non-edge-sensitive type IV neurons?

There was no clear difference between the distribution of BFs for rising-edge-sensitive and other units, shown in Figure 8A. The sampling of BFs was centered on frequencies from 8 to 20 kHz, which is the range of the lowest frequency notch in cat HRTFs (Musicant et al., 1990; Rice et al., 1992). Given this sample, there was no segregation of spectral edge responses by BF.

Edge sensitivity was strongly linked to the shape of BBN rate versus level functions. Most rising-edge-sensitive units had non-monotonic BBN rate–level functions, reflected in a negative local slope, as in Figures 2B and 3B. In contrast, notch-inhibited units had monotonic BBN rate–level functions with zero or positive slopes everywhere, as in Figure 6B. Figure 8B shows a scatter plot of the slope of BBN rate functions at sound levels just above their inflection point, measured as in Figure 8D. Edge-sensitive units tended to have intermediate values of negative slopes (shaded symbols), whereas notch-inhibited units had predominantly zero or positive slopes (open triangles). The difference is significant ($p < 0.0005$; rank-sum test). Notch-excited units also had negative slopes, more negative than those of edge-sensitive units (Fig. 8, × symbols) ($p < 0.05$, rank-sum test) (compare Fig. 7B with Figs. 2B, 3B).

One hypothesis for edge sensitivity is that it reflects an offset in the BFs of inhibitory inputs relative to excitatory inputs. The central inhibitory area (CIA) is the strong inhibitory frequency region centered near BF in the tone response maps of type IV units; the CIA corresponds to the type II inhibitory input (Voigt and Young, 1990; Spirou and Young, 1991). These previous studies have suggested that the CIA usually is centered below BF,

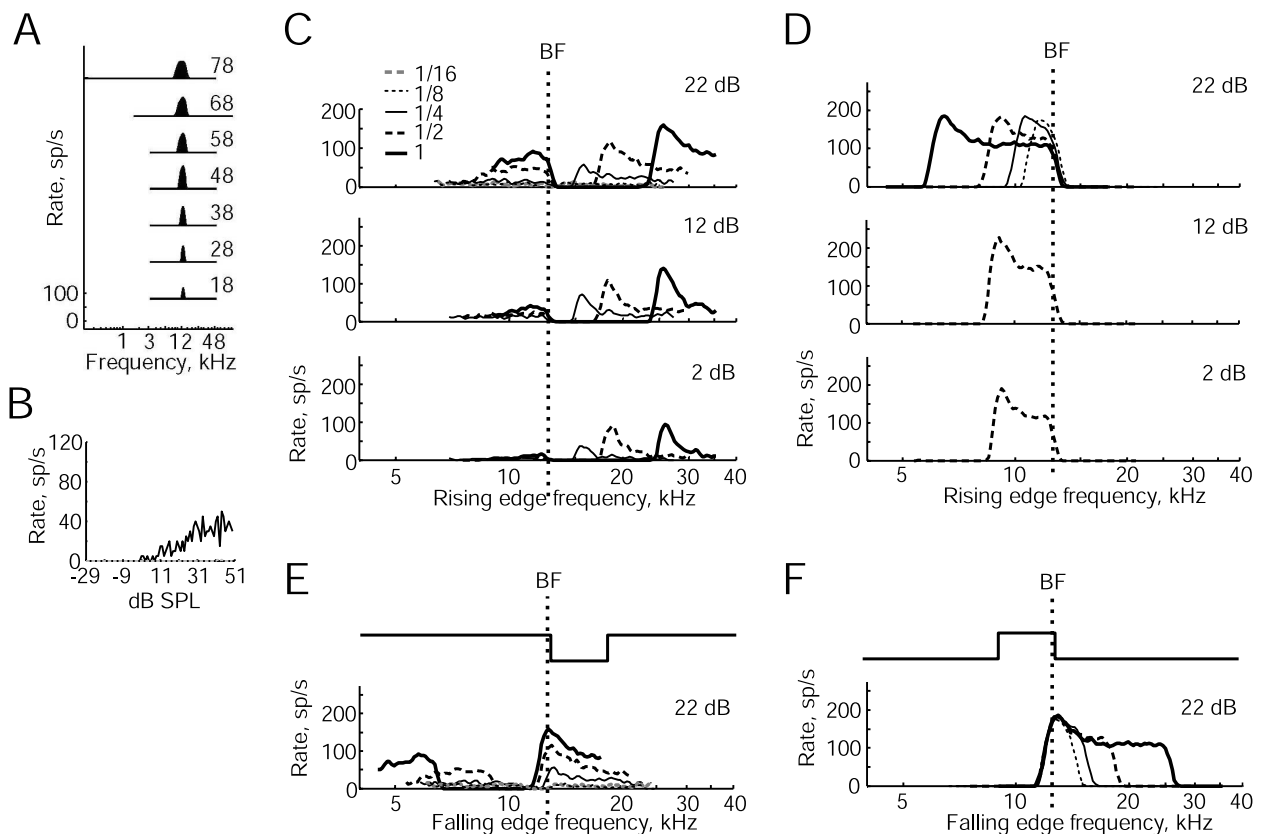


Figure 9. Example of a type II neuron (BF of 12.7 kHz). **A–D** are organized as in Figure 3. Spontaneous rate is not shown because it was zero. **E**, Responses to notch noise plotted versus falling edge frequencies to illustrate peaks when falling edges are near BF. **F**, Responses to band noise plotted versus falling edge frequencies. dB SPL, Decibels of sound pressure level; sp/s, spikes per second.

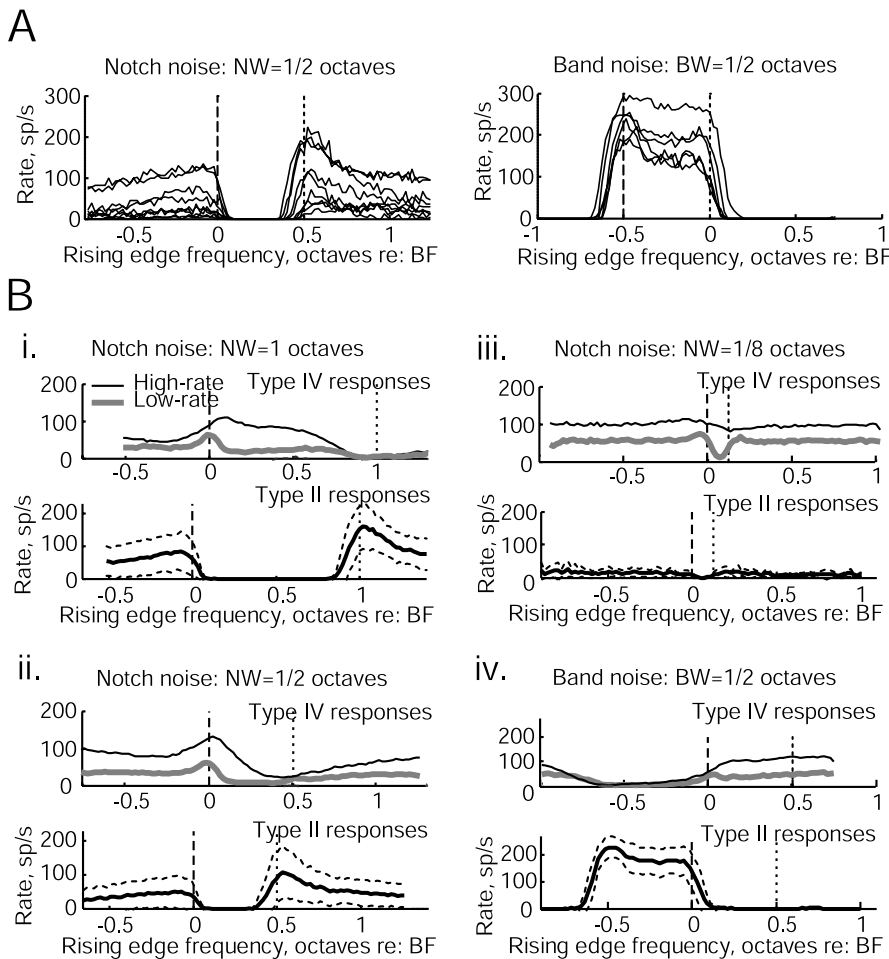


Figure 10. Superimposed and average population responses of type II units to notch and band noise sweeps and comparisons with average type IV responses. **A**, Superimposed notch noise sweep responses (left) and noise band sweep responses (right) show the population similarity of type II responses. **B**, Direct comparison of average type IV responses (top rows; low-rate, thick gray lines; high-rate, thin black lines) and type II responses (bottom rows; thick black lines) under various sweep conditions, with the type II response shifted down 0.1 octave in frequency to correspond to the measured frequency difference in Figure 8C. As in Figure 5B, dashed lines indicate 1 SD above and below average responses. NW, Notch width; BW, bandwidth; sp/s, spikes per second; re, relative to.

which is the offset needed to give rising edge sensitivity. The CIA center frequency (CIA CF) was calculated from tone response maps as the logarithmic center frequency of inhibition at the lowest sound level at which inhibition was seen, as by Spirou and Young (1991). As shown in Figure 8C, most edge-sensitive type IV units had CIA CFs below BF (shaded symbols), whereas notch-inhibited units had CIA CFs at or above BF (open triangles) ($p < 0.05$, rank-sum test). The notch-excited units, like the edge-sensitive units, had CIA CFs below BF (\times symbols).

Comparison of recording depths showed a difference in the locations of low-rate and high-rate neurons in the DCN. Recording depths were measured with the microdrive as the distance, in micrometers, from the surface of the DCN. There was no difference between the depth distributions of edge-sensitive versus non-edge-sensitive type IV units. However, there was a striking difference within the edge-sensitive group. Low-rate units occurred over a range of depths, but high-rate units occurred only at depths $>600 \mu\text{m}$. Many of the units came from different experiments, so this was not an effect attributable to one cat. In fact, the one track with both low- and high-rate units had the two low-rate units at shallower depths than the one high-rate unit. This difference in depth of low- and high-rate units is highly

significant ($p < 0.01$; exact Fisher's test) and suggests that neuroanatomical differences may accompany physiological differences between low- and high-rate type IV units, specifically that high-rate units are found in deep DCN, whereas low-rate units are found in both deep DCN and the pyramidal cell layer. Similarly, the notch-excited units were found at depths $>500 \mu\text{m}$. However, because the depth measurements were not normalized for track angle, nucleus size, or differences in shape, additional study followed by histological reconstruction would be useful to verify these trends.

Type II responses to notch noise and noise bands only explain some features of type IV responses

Type II units are a prominent inhibitory input to DCN type IV units (Voigt and Young, 1990). Although they are not considered to be a source of inhibition for noise notches centered at BF (Nelken and Young, 1994), their responses for notches centered away from BF have not been studied extensively.

We found that seven of seven type II neurons studied showed very similar, strongly modulated responses to notch noise and noise band sweeps (Fig. 9). This response modulation is consistent with previous type II data (Nelken and Young, 1994). These responses differed from the type IV responses described above in that peak responses were not seen at the rising band edge (Fig. 9C,D) but rather at the falling band edge (Fig. 9E,F). However, note that type II units responded to both edges, unlike rising edge-sensitive type IV units, which were inhibited by the falling edge.

These high-rate responses to notch noise seem inconsistent with previously described weak rate responses to BBN in type II units (Young and Voigt, 1982; Spirou et al., 1999). However, the data are consistent, as is shown by the observation that the excitatory responses decreased as notch width decreased, converging to the BBN response at very narrow notch widths.

Figure 10 shows a comparison of average type II and type IV responses to notches and noise bands. All of the type II responses studied at octave notch width are superimposed on a normalized frequency scale (Fig. 10A), and these are averaged and compared with type IV responses in Figure 10B. The type II frequency axes are shifted to lower frequencies relative to the type IV axes to reflect the empirically measured 0.1 octave frequency difference between CIA CFs and type IV BF (Fig. 8C). This frequency difference is consistent with the difference in BF between type II and type IV units showing cross-correlation evidence of an inhibitory synaptic connection (Voigt and Young, 1990).

Note that type II activity is qualitatively the inverse of the responses of the high-rate type IV group (Fig. 10B, thin black lines). For example, the strong inhibition of type II units when the notch is centered near BF corresponds to an increase in rate in the type IV units, especially noticeable for the widest notch

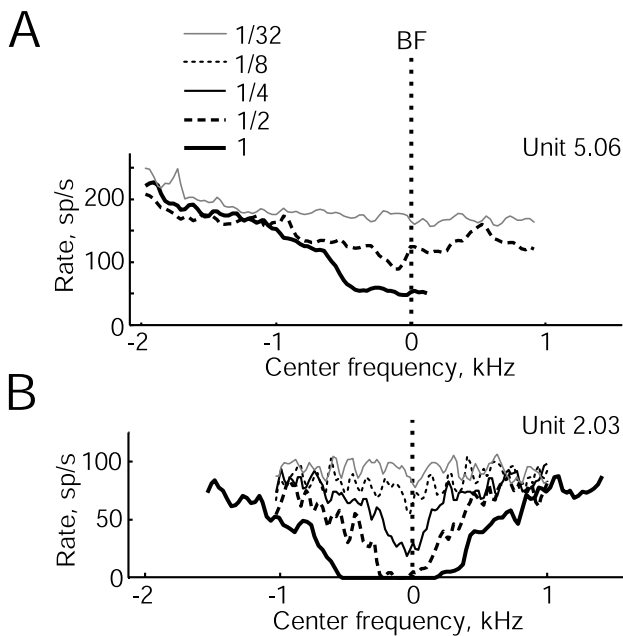


Figure 11. Examples of two onset-C responses to notch noise sweeps plotted versus notch center frequency. Spectral irregularities in the calibration were not compensated for in these early data. **A**, BF of 21.3 kHz. Pass-band level was 45 dB. Data are incomplete at high center frequencies because of sampling rate limitations. **B**, BF of 9.4 kHz. Pass-band level was -13 dB. Archival data are from Nelken and Young (1994). These stimuli differed slightly in that notches were centered linearly, not logarithmically, in frequency. sp/s, Spikes per second.

widths. Peaks in activity in type II units also correspond generally to decreases in rate in the high-rate type IV units. In particular, the broad peak responses to falling edges in type II units correspond to the inhibited responses to falling edges in type IV units (Fig. 10*Bi,Bii*, vertical dotted lines); this enhances the prominence of the peak responses to rising edges.

In contrast, the responses of the low-rate type IV units (Fig. 10*B*, thick gray lines) are very different from the predictions that follow from type II inhibition. Although the low-frequency side of the response peak at the rising band edge generally corresponds to a decrease in type II rate, there is no type II response feature that can be used to account for the high-frequency side of the peak. This is especially apparent at wide notch widths in which type II units do not respond at all to notch frequencies around BF (Fig. 10*Bi*). This unexplained inhibition, plus the general low-rate nature of these type IV responses, suggests the presence of additional inhibitory mechanisms.

It is also evident that the loss of edge sensitivity at small notch widths is attributable to the minimum notch width for type II activity. When the notch is narrow, the type II activity is greatly reduced and provides insufficient inhibition to shape the lower-frequency side of the peak (Fig. 10*Biii*).

Onset-C responses are consistent with broadband integration

Onset-C units in the VCN are characterized physiologically by strong responses to BBN and weak responses to tones (Smith and Rhode, 1989; Winter and Palmer, 1995); they are thought to be a wideband inhibitory input to the DCN (Nelken and Young, 1994; Winter and Palmer, 1995; Doucet and Ryugo, 1997). The responses of two onset-C units to notch noise sweeps are shown in Figure 11. Consistent with previous results showing these units to have excitatory inputs over a wide BF range (Jiang et al., 1996; Palmer et al., 1996; Arnott et al., 2004), they gave a broad excitatory response over a large range of notch frequencies, and the

response reached its minimum when the notch was centered at BF (Fig. 11). Also note that the responses were smaller for wide notch widths than for narrow notch widths. These characteristics are not the ones needed to account for the unexplained inhibition of low-rate type IV units shown in Figure 11*B*.

Simulation of DCN neurons replicates some aspects of rising edge sensitivity

The model of DCN type IV units developed by Hancock and Voigt (1999) was used to test whether the usually assumed two-inhibitor model of the DCN (Fig. 12*D*) is able to account for the responses to band edges. Figure 12*A* shows that the model successfully reproduces onset-C (assumed to be the WBI) (Fig. 12*Ab*) and type II (Fig. 12*Ac*) responses from simulations of the population response of AN fibers (Fig. 12*Aa*). The strong rate modulation of the WBI by notch frequency was obtained only with a smaller AN fiber integration bandwidth than that used by Hancock and Voigt (Table 1). The asymmetric response of type II units to falling, but not rising, band edges required both the strong WBI rate modulation and an assumed 0.3 octave offset in BF of the WBI units relative to type II units. Note also the increases in type II response as notch width increases, which reflect the weakening of the WBI response as total stimulus bandwidth decreases.

Type IV responses were simulated either without (Fig. 12*Be*) or with (Fig. 12*C*) the inhibitory connection from WBI units to type IV units. Type II BFs were offset 0.1 octaves lower in frequency relative to type IV BFs, as suggested by the data. Type II responses were generated with the WBI input and BF alignment as in Figure 12*A*.

Without WBI input, the type IV simulations exhibit rate peaks at the rising band edge (Fig. 12*B*, arrows). The vertical lines in Figure 12*B* make it clear that the peaks come about because of the offset in type II BFs. These type IV simulations resemble the high-rate type IV data (Fig. 5, green lines) but do not show the strong inhibitory responses seen in low-rate units (Fig. 5, brown lines) with the notch near BF.

Previously, the inhibitory responses to notches centered on BF were attributed to reduced rate in AN fibers and inhibitory inputs from the WBI (Nelken and Young, 1994; Hancock and Voigt, 1999). However, adding inhibitory inputs from the WBI does not produce appropriate responses in this model, as shown in Figure 12*C*. Model responses are shown for four inhibitory strengths of the WBI input to type IV units and are compared with averaged data from low-rate units responding to the same stimuli (heavy lines). Although the WBI inhibition reduces the discharge rates, it does not do so with the pattern seen in the data. The WBI inhibition is greatest at notch frequencies far from the type IV BF (Fig. 12*Ab*), in contrast to the inhibition seen in the data which is greatest at notch frequencies near the type IV BF.

The weak link in this modeling is that the WBI simulations are based on (1) limited onset-C data and (2) parameters that replicate type II behavior. It could be argued that type IV units might receive inputs from a different subset of onset-C units than type II units, or even other types of onset units, with wider integration bandwidths and flatter rate modulation by notch frequency. Such an input would respond with little modulation to narrow and wider notches, and, together with reduced AN excitation, might account for notch inhibition. However, it is not evident how such an input would compensate for spread of excitation with increased sound level. Furthermore, the inhibition in the data are strongest at rising edge frequencies just above type IV BF rather than when the notch is centered on BF, as would be expected if the

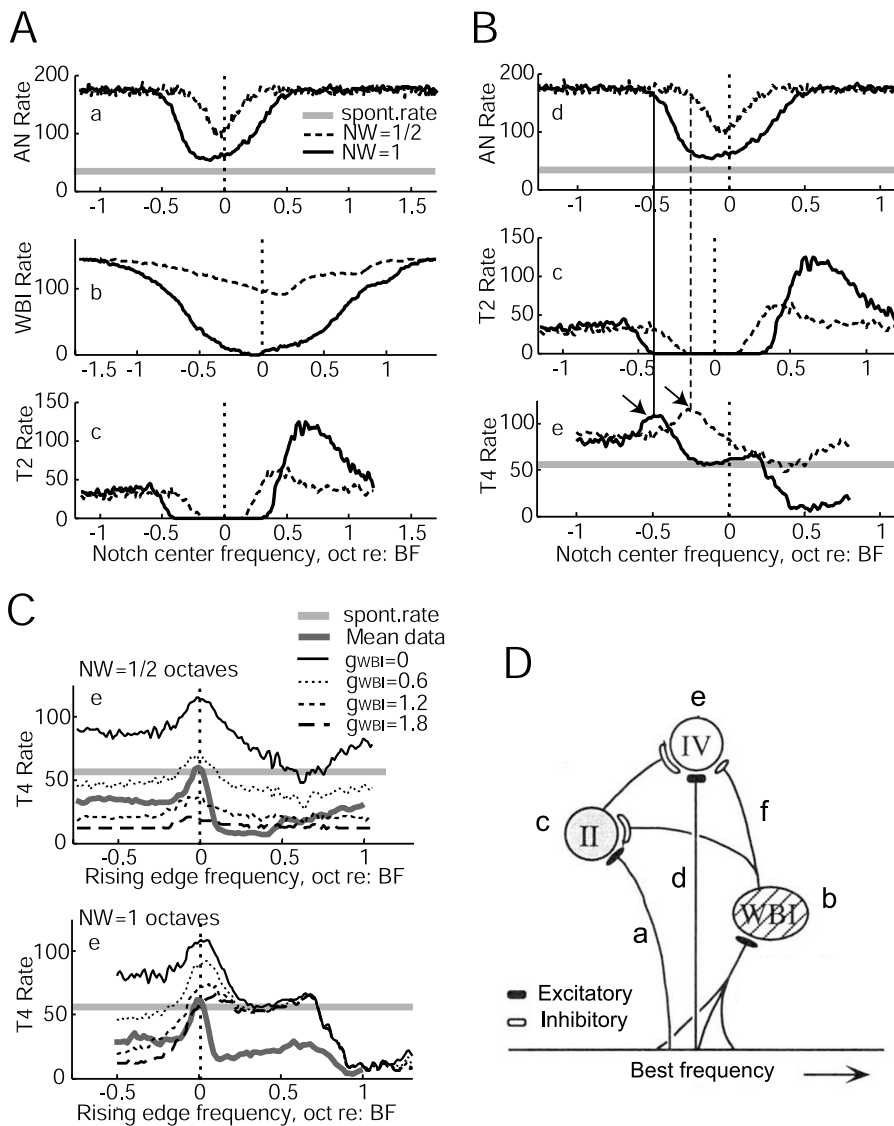


Figure 12. Simulations of AN, WBI, type II, and type IV responses to notch noise sweeps at spectrum levels of 0 dB. The hypothesized circuit of the DCN is shown in **D**. Lines show synaptic connections from neuron to neuron; excitatory and inhibitory terminals are shown as filled or unfilled, respectively. The strength of a synaptic connection is indicated by its size. The horizontal line marked “best frequency” shows the tonotopic array of auditory-nerve inputs to DCN; vertical lines show AN axons of different BFs connecting to neurons of the DCN circuit. Axons and cells are labeled with lowercase letters (a–f) in this circuit diagram for reference in **A–C**. **A**, Shaping of type II responses (**c**) by excitatory AN input (**a**) and inhibitory WBI input (**b**) for two notch widths. Strong modulation of WBI rate by notch frequency and an offset in WBI BF relative to AN BF (+0.3 octave) are sufficient to replicate the type II falling-edge rate peak. **B**, Shaping of the type IV response peak to rising spectral edges by a spectrally asymmetric combination of inhibitory type II input (**c**) and excitatory AN input (**d**) without WBI input. **C**, Effect of WBI input (**b**) to type IV for different WBI synapse strengths g_{WBI} , given as the conductance of the WBI input normalized by the resting conductance of the cell. For comparison, the type II inhibition has a g_{II} of 2.25. The mean data are shown for comparison. Addition of the WBI does not account for additional inhibition with the rising edge frequencies above BF, especially for wide notch widths. NW, Notch width; oct, octave; re., relative to; spont. rate, spontaneous rate; T2, type II; T4, type IV.

inhibition were attributable to general inhibition plus lack of AN excitation. This is most evident when looking at the difference between the low-rate and high-rate group responses for wider notch widths in Figure 5B. The difference is not as apparent at smaller notch widths because it overlaps with the type II inhibition, which clearly affects both the low- and high-rate groups.

Discussion

Physiological mechanisms of edge sensitivity

Three main groups of DCN type IV units have been defined on the basis of responses to notch noise: edge sensitive, notch inhib-

ited, and notch excited. The notch responses are correlated with other properties, such as responses to BBN and the relative positioning of the CIA with respect to unit BF. Although the properties of these unit types cannot be fully accounted for by our understanding of DCN circuitry, models that account for their general behavior can be offered. The notch-inhibited units (Fig. 6) have the simplest response properties. They show signs of only weak inhibitory inputs in response to noise, in that their BBN rate–level functions are monotonic (Figs. 6B, 8B) and they are inhibited by notch noise and excited by noise bands without edge sensitivity (Fig. 6C,D). Their notch noise properties are qualitatively consistent with the drop in discharge rate of their AN inputs attributable to the notch (Fig. 12Aa); only small additional inhibition seems necessary, for example, at the widest notch width in Figure 6C. Effects of type II inhibition are not obvious in these notch responses, perhaps because they are weak or because the CIA CF is not reliably offset from the BF of the unit (Fig. 8C). Of course, type II inhibition must be present in these units to account for their responses to tones (Fig. 6A).

The notch-excited units (Fig. 7) show behavior that varies with sound level. At higher levels, these units are excited when the notch is located near BF and inhibited by the noise band. This behavior is qualitatively the inverse of that shown by type II units (Fig. 9), suggesting that the main properties of the responses of notch-excited units reflect inhibition from type II units. At low sound levels, the type II units are not activated by the noise, and the notch-excited units are like notch-inhibited units. This model does not explain the strongly non-monotonic rate functions for BBN shown by these units (Figs. 7B, 8B), suggesting that these units may have an additional inhibitory input that responds strongly to BBN. This could be from the WBI (Fig. 11), which would be consistent with the notch and band responses of these units, or from another source.

The edge-sensitive units divide into two subclasses, called low- and high-rate. Both groups show moderately nonmonotonic responses to BBN (Fig. 8B) and an offset toward lower frequencies of their CIA CFs (Fig. 8C). The latter property was used in Figures 10 and 12 to account for the general properties of the high-rate subclass. The main effect controlling the responses of type IV units in the model is the inhibitory input from type II units. The rate peak with a rising band edge at BF is produced by this model, but the shift toward higher frequencies of the rate peak as notch width increases is not (Fig. 5B). There is also a shift with sound level (Fig. 5C), which could

not be investigated with the model because of its limitations to low sound levels. Moreover, it seems clear that an additional inhibitory mechanism, discussed below, is necessary to account for the properties of the low-rate units.

The peak shifts in the high-rate units with sound level (Fig. 5C) might be caused by an increase in the AN discharge rate with sound level for BFs within the notch. Such a rate increase is expected from the rate responses of AN fibers to broadband stimuli (Schalk and Sachs, 1980) and would not be opposed by type II inhibition, because type II units are inhibited at similar BFs (Fig. 9C). However, this explanation does not account for the shift in peak locations with increases in notch width.

The additional inhibitory input

Previously, the additional inhibitory input needed to account for low-rate edge-sensitive neurons was assumed to be the WBI (Nelken and Young, 1994; Blum and Reed, 1998; Hancock and Voigt, 1999). Whereas simulations were able to model inhibitory responses to notches centered on BF using the WBI, the responses to the wider array of notch positions used here were not studied and cannot be simulated with this model.

The properties of the additional inhibitory source can be inferred from the data in Figure 5 as the difference between the green and brown lines in Figure 5B, taking into account the effects of the type II input, shown in Figure 10B. The additional inhibitory input should respond when the BF of the type IV unit is within the notch, especially with the rising edge of the notch just above BF.

Two candidates for the additional inhibitory source among the unit types studied in this paper are the notch-excited units and the high-rate edge-sensitive units. Both types give responses that are qualitatively like the inferred additional inhibitory input. However, both types are type IV units, and the existing evidence suggests that type IV units are DCN principal cells (Young, 1984) and not interneurons. There is some evidence that principal cells give recurrent collaterals in cat (Smith and Rhode, 1985), making it feasible that type IV units could interact with other type IV units in the DCN. Whereas DCN principal cells are generally negative for inhibitory neurotransmitters, there are reports of several large cells, including giant cells, in deep DCN that stain for glycine in the cat (Osen et al., 1990). It is possible that the notch-excited or high-rate type IV units, which electrode track locations suggest to be located in the deep DCN, correspond to these glycinergic cells and that these cells inhibit the low-rate type IV units. Another possibility is that the recurrent collaterals activate small inhibitory interneurons, which then terminate on low-rate type IV units.

Of course, the DCN receives inhibitory inputs from a variety of loci in the superior olive (Ostapoff et al., 1997) and inferior colliculus (Shore et al., 1991; Malmierca et al., 1996), which could provide the additional inhibitory input. At present, nothing is known about the notch noise responses of these neurons, except for the type O units in the inferior colliculus, which show responses to rising band edges (Davis et al., 2003) and could provide the additional inhibitory input, either directly or indirectly.

Encoding of spectral edges and notches

Previous physiological studies in anesthetized cats using sounds in the free field have shown that DCN responses carry information about sound location (Imig et al., 2000). Those studies focused on the inhibitory responses, but some of their data also show excitatory peaks adjacent to the null responses (Fig. 12). The excitatory peaks are not large in the examples shown. How-

ever, sound locations were only sampled at 22.5° intervals in elevation, corresponding to $\sim 1/4$ octave steps in spectral notch frequency near the midline. Here, the rate peaks were $\sim 1/10$ octave wide, so they would have been incompletely sampled by Imig et al. (2000).

These DCN results are similar to results for type O neurons in the ICC (Davis et al., 2003). Type O neurons respond with a peak of discharge rate when the rising edge of a notch noise is aligned near BF. The results shown here suggest that edge sensitivity in the ICC results from edge sensitivity of inputs from the DCN, which are an important excitatory input to type O neurons (Davis, 2001). However, the edge sensitivity is elaborated in the ICC, in that type O neurons respond less to noise bands than to notch noise, and a full model of type O neurons requires inputs in addition to DCN type IV units (Davis et al., 2003).

Psychophysical studies

These results are consistent with observations in human psychophysical studies suggesting that perceived sound location is influenced by the frequency location of the rising spectral edge of notch noise, noise bands, or high-pass noise, as long as the rising spectral edge is in the physiological range of rising edge frequencies in human HRTFs (Middlebrooks, 1992; Macpherson and Middlebrooks, 1999). This illusion is robust for notch widths of $2/3$ or 1 octaves but not $1/3$ octave (Macpherson and Middlebrooks, 1999), consistent with the increasing amplitude of the rate peak as the notch width increases (Figs. 2D, 3C).

In cats, illusory vertical locations produced by the simultaneous presentation of two sounds from two different spatial locations tends to be higher than predicted by a model based on the center frequency of the spectral notch (Tollin and Yin, 2003). However, the method used in those experiments produces notches in the sound spectrum at the eardrum that are wider and shallower than those in actual HRTFs, for the same notch frequencies. A rising spectral edge model predicts a higher illusory elevation for this HRTF than a spectral notch model. Thus, spectral edge sensitivity may explain the discrepancy between the predicted and perceived elevations in that study. However, additional work is needed to determine the effects of varying notch parameters, such as slope and depth, in both physiology and psychophysics.

References

- Arnott RH, Wallace MN, Shackleton TM, Palmer AR (2004) Onset neurons in the anteroventral cochlear nucleus project to the dorsal cochlear nucleus. *J Assoc Res Otolaryngol* 5:153–170.
- Blauert J (1969) Sound localization in the median plane. *Acustica* 22:205–213.
- Blum JJ, Reed MC (1998) Effects of wide band inhibitors in the dorsal cochlear nucleus. II. Model calculations of the responses to complex sounds. *J Acoust Soc Am* 103:2000–2009.
- Bruce IC, Sachs MB, Young ED (2003) An auditory-periphery model of the effects of acoustic trauma on auditory nerve responses. *J Acoust Soc Am* 113:369–388.
- Davis KA (2001) Evidence of a functionally segregated pathway from dorsal cochlear nucleus to inferior colliculus. *J Neurophysiol* 87:1824–1835.
- Davis KA, Ramachandran R, May BJ (2003) Auditory processing of spectral cues for sound localization in the inferior colliculus. *J Assoc Res Otolaryngol* 4:148–163.
- Doucet JR, Ryugo DK (1997) Projections from the ventral cochlear nucleus to the dorsal cochlear nucleus in rats. *J Neurophysiol* 83:926–940.
- Hancock KE, Voigt HF (1999) Wideband inhibition of dorsal cochlear nucleus type IV units in cat: a computational model. *Ann Biomed Eng* 27:73–87.
- Hebrank J, Wright D (1974) Spectral cues used in the localization of sound sources on the median plane. *J Acoust Soc Am* 56:935–938.

- Hellstrom LI (1998) Physiological responses to the pulsation threshold paradigm. I. Pulsation threshold patterns do not reproduce physiological rate profiles of high-pass and low-pass noise maskers. *J Acoust Soc Am* 85:230–242.
- Huang AY, May BJ (1996) Sound orientation behavior in cats. II. Mid-frequency spectral cues for sound localization. *J Acoust Soc Am* 100:1070–1080.
- Imig TJ, Bibikov NG, Poirier P, Samson FK (2000) Directionality derived from pinna-cue spectral notches in cat dorsal cochlear nucleus. *J Neurophysiol* 83:907–925.
- Jiang D, Palmer AR, Winter JM (1996) The frequency extent of two-tone facilitation in onset units in the ventral cochlear nucleus. *J Neurophysiol* 75:380–395.
- Macpherson EA, Middlebrooks JC (1999) Sound localization illusions produced by source spectrum discontinuities. *Assoc Res Otolaryngol Abstr*, 22nd meeting, abstract 112.
- Malmierca MS, Le Beau FE, Rees A (1996) The topographical organization of descending projections from the central nucleus of the inferior colliculus in guinea pig. *Hear Res* 93:167–180.
- May BJ (2000) Role of the dorsal cochlear nucleus in the sound localization behavior of cats. *Hear Res* 148:74–87.
- Middlebrooks JC (1992) Narrow-band sound localization related to external ear acoustics. *J Acoust Soc Am* 87:2188–2200.
- Musicant AD, Chan JC, Hind JE (1990) Direction-dependent spectral properties of cat external ear: new data and cross-species comparisons. *J Acoust Soc Am* 87:757–781.
- Nelken I, Young ED (1994) Two separate inhibitory mechanisms shape the responses of dorsal cochlear nucleus type IV units to narrowband and wideband stimuli. *J Neurophysiol* 71:2446–2462.
- Oertel D, Young ED (2004) What's a cerebellar circuit doing in the auditory system? *Trends Neurosci* 27:104–110.
- Osen KK, Ottersen OP, Storm-Mathisen J (1990) Colocalization of glycine-like and GABA-like immunoreactivities. A semiquantitative study of individual neurons in the dorsal cochlear nucleus of cat. In: *Glycine neurotransmission* (Ottersen OP, Storm-Mathisen J, eds), pp 417–451. New York: Wiley.
- Ostapoff EM, Benson CG, Saint Marie RL (1997) GABA- and glycine-immunoreactive projections from the superior olivary complex to the cochlear nucleus in guinea pig. *J Comp Neurol* 381:500–512.
- Palmer AR, Jiang D, Marshall DH (1996) Responses of ventral cochlear nucleus onset and chopper units as a function of signal bandwidth. *J Neurophysiol* 75:780–795.
- Rice JJ, May BJ, Spirou GA, Young ED (1992) Pinna-based spectral cues for sound localization in cat. *Hear Res* 58:132–152.
- Schalk TB, Sachs MB (1980) Nonlinearities in auditory-nerve fiber responses to bandlimited noise. *J Acoust Soc Am* 67:903–913.
- Shofner WP, Young ED (1985) Excitatory/inhibitory response types in the cochlear nucleus: relationships to discharge patterns and responses to electrical stimulation of the auditory nerve. *J Neurophysiol* 54:917–939.
- Shore SE, Helfert RH, Bledsoe Jr SC, Altschuler RA, Godfrey DA (1991) Descending projections to the dorsal and ventral divisions of the cochlear nucleus in guinea pig. *Hear Res* 52:255–268.
- Smith PH, Rhode WS (1985) Electron microscopic features of physiologically characterized, HRP-labeled fusiform cells in the cat dorsal cochlear nucleus. *J Comp Neurol* 237:127–143.
- Smith PH, Rhode WS (1989) Structural and functional properties distinguish two types of multipolar cells in the ventral cochlear nucleus. *J Comp Neurol* 282:595–616.
- Spirou GA, Young ED (1991) Organization of dorsal cochlear nucleus type IV unit response maps and their relationship to activation by band limited noise. *J Neurophysiol* 65:1750–1768.
- Spirou GA, Davis KA, Nelken I, Young ED (1999) Spectral integration by type II interneurons in dorsal cochlear nucleus. *J Neurophysiol* 82:648–663.
- Sutherland DP, Masterton RB, Glendenning KK (1998) Role of acoustic striae in hearing: reflexive responses to elevated sound sources. *Behav Brain Res* 97:1–12.
- Tollin DJ, Yin CT (2003) Spectral cues explain illusory effects with stereo sounds in cats. *J Neurophysiol* 90:525–530.
- Voigt HF, Young ED (1990) Cross-correlation analysis of inhibitory interactions in dorsal cochlear nucleus. *J Neurophysiol* 64:1590–1610.
- Winter IM, Palmer AR (1995) Level dependency of cochlear nucleus onset unit responses and facilitation by second tones or broadband noise. *J Neurophysiol* 73:141–159.
- Young ED (1984) Response characteristics of neurons of the cochlear nuclei. In: *Hearing science, recent advances* (Berlin CI, ed), pp 423–460. San Diego: College-Hill.
- Young ED, Brownell WE (1976) Responses to tones and noise of single cells in the dorsal cochlear nucleus of unanesthetized cats. *J Neurophysiol* 39:282–300.
- Young ED, Davis KA (2002) Circuitry and function of the dorsal cochlear nucleus. In: *Integrative functions in the mammalian auditory pathway* (Oertel D, Fay RR, Popper AN, eds), pp 160–206. New York: Springer.
- Young ED, Voigt HF (1982) Response properties of type II and type III units in dorsal cochlear nucleus. *Hear Res* 6:153–169.
- Zhang X, Heinz MG, Bruce IC, Carney LH (2001) A phenomenological model for the responses of auditory nerve fibers. I. Nonlinear tuning with compression and suppression. *J Acoust Soc Am* 109:648–670.